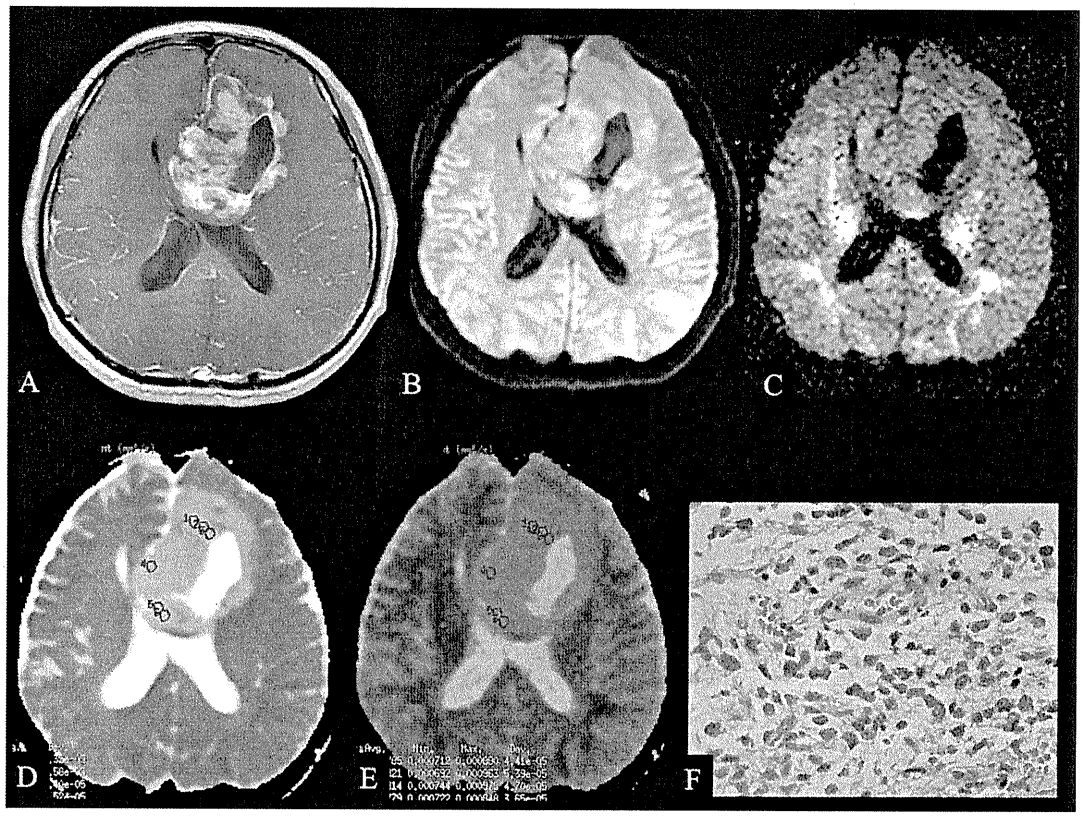

Fig. 2. Glioblastoma in a 58-year-old man. (A) Axial contrast-enhanced T1-weighted image shows diffuse tumor enhancement in the left temporal lobe. (B) Axial DWI at *b*-1000 s/mm^2 shows tumor isointensity. (C) Axial DWI at *b*-4000 s/mm^2 shows tumor hyperintensity. (D) Axial ADC map at *b*-4000 s/mm^2. (E) Axial ADC map at *b*-1000 s/mm^2. (F) Photomicrograph of hematoxylin–eosin stained tumor tissue.

1000 and *b*-4000. Of 14 glioblastomas, 7 were high-intense at *b*-1000 and 9 were high-intense at *b*-4000. Analysis by Student's *t*-test showed that the ADC values of glioblastoma were statistically higher than of lymphoma (supplemental figure). Among the 3 ADC value categories, the absolute *t*-value was largest for ADC_{MIN} at *b*-4000. Comparison among ADC_{MEAN}, ADC_{MIN}, and ADC_{MAX} at *b*-4000 using log-likelihood criteria showed that ADC_{MIN} at *b*-4000 discriminated most accurately (data not shown).

3.4. Cellularity and ADC value of tumor tissue

We found a negative correlation between tumor cellularity and the ADC of tumors (Fig. 5). Mean cell density per field was 450 (range 302–619) for lymphomas and 311 (range 143–577) for glioblastomas. Compared to the correlation ($r = -0.600$, $p = 0.0019$) between the cytoplasm and ADC_{MIN} at *b*-1000, a stronger negative correlation ($r = -0.707$, $p = 0.0001$) was obtained at *b*-4000.

4. Discussion

Ours is the first documentation that calculation of the ADC based on a high *b*-value (*b*-4000) at 3 T MRI more effectively distinguishes between lymphoma and glioblastoma than the ADC obtained with the standard *b*-value (*b*-1000).

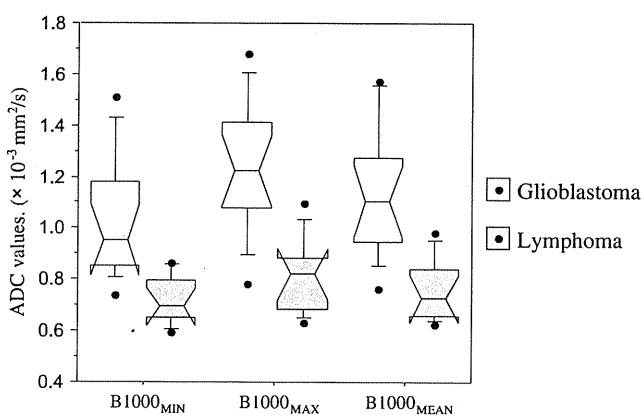

Fig. 3. Box plots of ADC values at *b* = 1000 s/mm^2. The values of ADC_{MIN} ($B1000_{MIN}$), ADC_{MAX} ($B1000_{MAX}$), and ADC_{MEAN} ($B1000_{MEAN}$) for lymphoma and glioblastoma are shown.

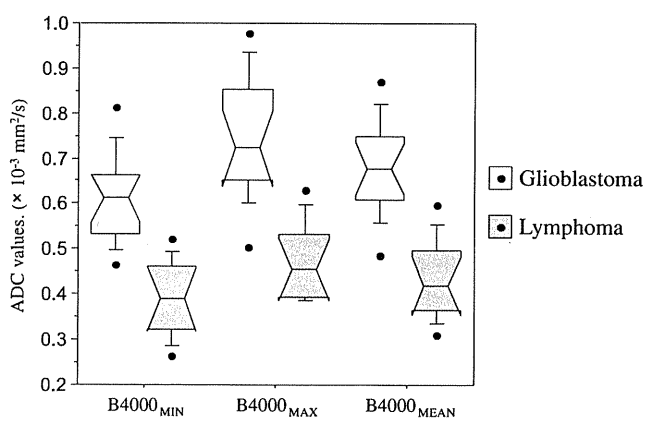

Fig. 4. Box plots of ADC values at *b* = 4000 s/mm^2. The values of ADC_{MIN} ($B4000_{MIN}$), ADC_{MAX} ($B4000_{MAX}$), and ADC_{MEAN} ($B4000_{MEAN}$) for lymphoma and glioblastoma are shown.

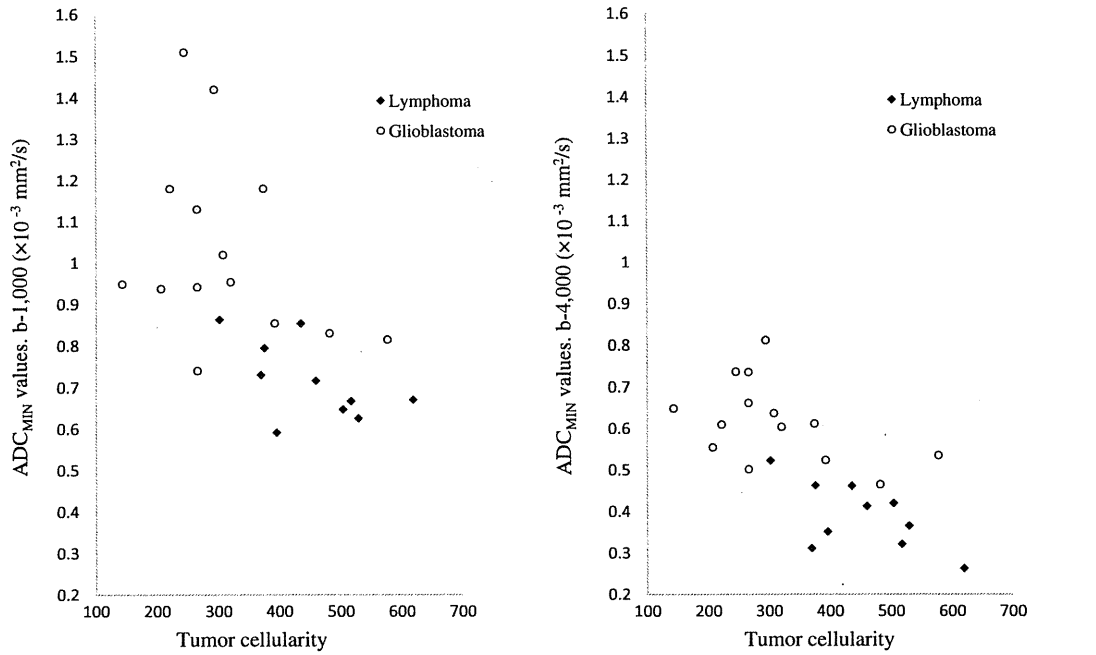

Fig. 5. Scatterplots of the minimum apparent diffusion coefficient values at *b*-1000 s/mm^2 versus tumor cellularity (left) and minimum ADC values at *b*-4000 s/mm^2 versus tumor cellularity (right).

In our study, the ADC_{MIN}, ADC_{MEAN}, and ADC_{MAX} values of lymphoma obtained from DWI at *b*-1000 were consistently lower than of glioblastoma. In other studies [4,8,10–12], the ADC_{MEAN} at *b*-1000 ranged from 0.580 to 0.750 × 10^{-3} mm^2/s in patients with lymphoma and from 0.963 to 1.140 × 10^{-3} mm^2/s in patients with glioblastoma; our results are consistent with these studies. However, according to earlier investigations, the difference between the ADC of glioblastoma and lymphoma was not statistically significant although the ADC of lymphomas was lower than of high-grade gliomas [12]. In fact, the overlapping of the ADC values rendered the differentiation between lymphoma and glioblastoma based on the ADC difficult [8,9,12]. In those studies, DWI scans were performed with a 1.5 T scanner at *b*-1000 [4,7–10,12]; the use of MR instruments with a higher static magnetic field and a powerful gradient unit may improve the differentiation between glioblastoma and lymphoma.

Our study using a high *b*-value confirmed that the ADC obtained at *b*-4000 was statistically significantly lower for lymphoma than glioblastoma and the statistical difference was larger at *b* = 4000 than *b* = 1000 s/mm^2. The overlap in all ADC values of lymphoma and glioblastoma decreased for all ADC measurements, especially ADC_{MIN}, at *b*-4000 compared to *b*-1000. Our findings that DWI and ADC calculations based on high *b*-values yield better results coincide with earlier reports [16–20].

On visual inspection, all lymphomas were high-intense on DWI at *b*-1000 and *b*-4000; 7 of 14 glioblastomas were high-intense and 7 were iso-intense at *b*-1000. On DWI scans, 2 of the 7 glioblastomas that were iso-intense at *b*-1000 became high-intense at *b*-4000, the other 5 remained iso-intense, suggesting the involvement of a greater diffusion-weighted response and a lower T2 shine-through effect at the higher *b*-value [16].

We focused on tumors that were high-intense on DWI scans and analyzed the ADC value of glioblastomas and lymphomas with high DWI signal intensity because this type of information is clinically relevant. This analysis confirmed that among the 3 ADC categories, ADC_{MIN} obtained from DWI at *b*-4000 differentiated most accurately between lymphomas and glioblastomas.

Comparisons between the ADC at *b*-1000 and cellularity in lymphomas and high-grade astrocytomas suggested that high cellularity leads to more restricted diffusion [4–7]. Others [21] also reported an inverse correlation between tumor cellularity and the ADC of meningiomas and gliomas. The results of our study are consistent with the observation that the ADC is inversely associated with tumor cellularity. Moreover, we present statistical evidence that tumor cellularity is inversely correlated with the ADC obtained at *b*-4000 DWI and that this inverse correlation is stronger than at *b*-1000.

At *b* = 1000 s/mm^2, diffusion within brain tissue is thought to be mono-exponential while at increased *b*-values up to 4000 s/mm^2 the response becomes bi-exponential [20,22]. There are slow- and fast diffusion components; they correspond with intra- and extracellular diffusion, respectively. As the fast component dominates at relatively low *b*-values (<1000 s/mm^2), the ADC values primarily reflect fast diffusion and thus the amount of extracellular space in the tumor [6,22]. Therefore, the inverse correlation between the cellularity of the tumor and the ADC at *b*-1000 may be due to variations in extracellular water diffusivity [4,6].

Studies on multi-component diffusion in brain tissue demonstrated that the slow component on high *b*-value DWI is more sensitive than on *b*-1000 DWI [15,16,19,23], an observation that supports our finding that the ADC based on higher *b*-values reflects changes in tumor cellularity more accurately. Explanations for the slow diffusion components present in brain tissue have been offered. Maier et al. [23] reported characteristic changes in bi-exponential diffusion parameters; they speculated that the slower diffusion component reflects the concentration of water-bound macromolecules, the cell size, and the tortuosity of the extracellular space. Thus, an increase in tissue tortuosity may progress in parallel with an increase in the extracellular space of malignant lesions [24]. However, the exact reason why the ADC at higher *b*-values manifests a better correlation with tumor cellularity is not known. In future studies we plan to use different types of tumor- and normal tissue to understand the effect of different *b*-values on ADC values and we will compare our findings with the histological features of the tissues.

There are some limitations in our study. Contributions from bulk capillary flow, active transport mechanisms, and the partial volume effect may affect ADC measurements. We compared T1- and T2-weighted-, FLAIR-, and Gd-enhanced T1- and T2*-weighted images in each case very carefully and placed the ROI centrally within the tumor area to avoid partial volume effects. However, structural heterogeneity due to micronecroses, microcysts, and microhemorrhages may remain undetected on MR images of brain tumors. Furthermore, the placement of ROIs is especially likely to result in variations in ADC measurements, resulting in apparently contradictory results among studies [25]. Therefore, the use of an ADC ratio for standardization purposes in which the ADC of a tumor would be compared with the ADC of a contralateral normal white matter region has been suggested [4,10–12]. However, the contribution to the ratio of the normal-appearing white matter depends on whether the ADC is affected by aging and the lesion per se [26]. We confirmed that *b*-4000 was useful for the differentiation between glioblastoma and lymphoma, however, the optimal *b*-value for a differential diagnosis of brain tumors remains unknown. Lastly, our study population was small and unequivocal results require the assessment of DWI scans and ADC values obtained at high *b*-values in larger prospective studies.

In conclusion, we confirmed an inverse correlation between the cellularity and the ADC of tumors. Based on the findings reported here we conclude that calculation of the ADC is useful for distinguishing lymphoma from glioblastoma. Although all ADC values of lymphoma were lower than of glioblastoma, there was a considerable overlap at *b*-1000. Because the ADC_{MIN} at *b*-4000 at 3 T MRI manifested the lowest degree of overlapping and a better inverse correlation reflective of tumor cellularity, it is useful for the preoperative acquisition of a correct differential diagnosis between lymphoma and glioblastoma.

Conflict of interest

None of the authors has to disclose any conflicts.

Acknowledgements

We thank Ursula Petralia for editorial review. This study was partially supported by a Grant-in-Aid for Scientific Research (C) and Grants-in-Aid from the Japan Society for the Promotion of Science (Grant No. 22591612).

Appendix A. Supplementary data

Supplementary data associated with this article can be found, in the online version, at doi:10.1016/j.ejrad.2010.11.005.

References

[1] DeAngelis LM. Brain tumors. N Engl J Med 2001;344:114–23.
[2] Schultz CJ, Bovi J. Current management of primary central nervous system lymphoma. Int J Radiat Oncol Biol Phys 2010;76:666–78.
[3] Traweek TS. Nervous system involvement by lymphoma, leukemia and other hematopoietic cell proliferation. In: Bigner DD, McLendon RE, Bruner JM, editors. Russell and Rubinstein's pathology of tumors of the nervous system, vol. 2, 6th ed. London: Arnold; 1998. p. 195–237.
[4] Guo AC, Cummings TJ, Dash RC, Provenzale JM. Lymphomas and high-grade astrocytomas: comparison of water diffusibility and histologic characteristics. Radiology 2002;224:177–83.
[5] Sugahara T, Korogi Y, Kochi M, et al. Usefulness of diffusion-weighted MRI with echo-planar technique in the evaluation of cellularity in gliomas. J Magn Reson Imaging 1999;9:53–60.
[6] Gupta RK, Cloughesy TF, Sinha U, et al. Relationships between choline magnetic resonance spectroscopy, apparent diffusion coefficient and quantitative histopathology in human glioma. J Neurooncol 2000;50:215–26.
[7] Barajas Jr RF, Rubenstein JL, Chang JS, Hwang J, Cha S. Diffusion-weighted MR imaging derived apparent diffusion coefficient is predictive of clinical outcome in primary central nervous system lymphoma. AJNR Am J Neuroradiol 2010;131:60–6.
[8] Yamasaki F, Kurisu K, Satoh K, et al. Apparent diffusion coefficient of human brain tumors at MR imaging. Radiology 2005;235:985–91.
[9] Kitis O, Altay H, Calli C, Yunten N, Akalin T, Yurtseven T. Minimum apparent diffusion coefficients in the evaluation of brain tumors. Eur J Radiol 2005;55:393–400.
[10] Horger M, Fenchel M, Nagele T, et al. Water diffusivity: comparison of primary CNS lymphoma and astrocytic tumor infiltrating the corpus callosum. AJR Am J Roentgenol 2009;193:1384–7.
[11] Toh CH, Castillo M, Wong AMC, et al. Primary cerebral lymphoma and glioblastoma multiforme: differences in diffusion characteristics evaluated with diffusion tensor imaging. AJNR Am J Neuroradiol 2008;29:471–5.
[12] Server A, Kulle B, Maehlen J, et al. Quantitative apparent diffusion coefficients in the characterization of brain tumors and associated peritumoral edema. Acta Radiol 2009;50:682–9.
[13] Schmierer K, Parkes HG, So PW, et al. High field (9.4 Tesla) magnetic resonance imaging of cortical grey matter lesions in multiple sclerosis. Brain 2010:1–10.
[14] Schepkin VD, Brey WW, Gor'kov PL, Grant SC. Initial in vivo rodent sodium and proton MR imaging at 21.1 T. Magn Reson Imaging 2010;28:400–7.
[15] Alvarez-Linera J, Benito-Leĭon J, Escribano J, Ray G. Predicting the histopathological grade of cerebral gliomas using high-*b*-value MR DW imaging at 3-Tesla. J Neuroimaging 2008;18(3):276–81.
[16] Seo HS, Chang KH, Na DG, Kwon BJ, Lee DH. High *b*-value diffusion ($b = 3000\ s/mm^2$) MR imaging in cerebral gliomas at 3 T: visual and quantitative comparisons with $b = 1000\ s/mm^2$. AJNR Am J Neuroradiol 2008;29:458–63.
[17] Doskaliyev A, Yamasaki F, Saito T, et al. Advantages of high *b* value diffusion-weighted imaging in the diagnosis of acute stroke – a case report. Cerebrovasc Dis 2009;27:616–7.
[18] Cihangiroglu M, Citci B, Kilickesmez O, et al. The utility of high *b*-value DWI in evaluation of ischemic stroke at 3 T. Eur J Radiol (2009), doi:10.1016/j.ejrad.2009.10.011.
[19] Yoshiura T, Mihara F, Tanaka A, et al. High *b* value diffusion-weighted imaging is more sensitive to white matter degeneration in Alzheimer's disease. Neuroimage 2003;20:413–9.
[20] DeLano MC, Cooper TG, Siebert JE, Potchen MJ, Kuppusamy K. High-*b*-value diffusion-weighted MR imaging of adult brain: image contrast and apparent diffusion coefficient map features. AJNR Am J Neuroradiol 2000;21:1830–6.
[21] Kono K, Inoue Y, Nakayama K, et al. The role of diffusion-weighted imaging in patients with brain tumors. AJNR Am J Neuroradiol 2001;22:1081–8.
[22] Niendorf T, Dijkhuizen RM, Norris DG, van Lookeren Campagne M, Nicolay K. Biexponential diffusion attenuation in various states of brain tissue: implications for diffusion-weighted imaging. Magn Reson Med 1996;36:847–57.
[23] Maier SE, Bogner P, Bajzik G, et al. Normal brain and brain tumor: multicomponent apparent diffusion coefficient line scan imaging. Radiology 2001;219:842–9.
[24] Vargova L, Homola A, Zamecnik J, Tichny M, Benes V, Sykova E. Diffusion parameters of the extracellular space in human gliomas. Glia 2003;42:77–88.
[25] Bilgili Y, Unal B. Effect of region of interest on interobserver variance in apparent diffusion coefficient measures. AJNR Am J Neuroradiol 2004;25:108–11.
[26] Rovaris M, Iannucci G, Cercignani M, et al. Age-related changes in conventional, magnetization transfer, and diffusion-tensor MR imaging findings: study with whole-brain tissue histogram analysis. Radiology 2003;227:731–8.

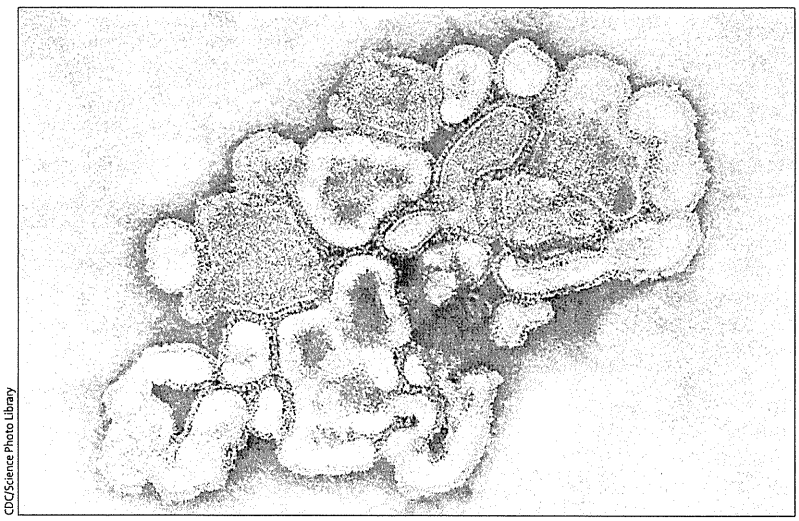

CDC/Science Photo Library

Coloured transmission electron micrograph of swine influenza virus particles

greater positive predictive value than did measurement of 14-3-3 concentrations alone. Collectively, the authors suggest that these brain-derived proteins have great diagnostic value in the assessment of possible sporadic Creutzfeldt-Jakob disease. This information will be useful to clinicians in the assessment of patients with this challenging diagnosis.

Emergence of the 2009 H1N1 influenza virus emphasises the ongoing challenges that infectious pathogens present. The coming years will undoubtedly continue to produce progress in understanding of the pathophysiological changes underlying neurological illness attributable to influenza and other pathogens, treatment and management approaches to bacterial meningitis, and diagnostic approaches to Creutzfeldt-Jakob disease and other neurological infections.

James J Sejvar
Division of High-Consequence Pathogens and Pathology and Division of Vector-Borne Infectious Diseases, National Center for Emerging and Zoonotic Infectious Diseases, Centers for Disease Control and Prevention, Atlanta, GA 30033, USA
jsejvar@cdc.gov

I declare that I have no conflicts of interest.

1 Davis LE. Neurologic and muscular complications of the 2009 influenza A (H1N1) pandemic. *Curr Neurol Neurosci Rep* 2010; **10:** 476–83.
2 Ekstrand JJ, Herbener A, Rawlings J, et al. Heightened neurologic complications in children with pandemic H1N1 influenza. *Ann Neurol* 2010; **68:** 762–66.
3 Schonberger LB, Bregman DJ, Sullivan-Bolyai JZ, et al. Guillain-Barré syndrome following vaccination in the National Influenza Immunization Program, United States, 1976–1977. *Am J Epidemiol* 1979; **110:** 105–23.
4 Centers for Disease Control and Prevention. Preliminary results: surveillance for Guillain-Barré syndrome after receipt of influenza A (H1N1) 2009 monovalent vaccine—United States, 2009–2010. *MMWR Morb Mortal Wkly Rep* 2010; **59:** 657–61.
5 Brouwer MC, Heckenberg SG, de Gans J, Spanjaard L, Reitsma JB, van de Beek D. Nationwide implementation of adjunctive dexamethasone therapy for pneumococcal meningitis. *Neurology* 2010; **75:** 1533–39.
6 Chohan G, Pennington C, Mackenzie JM, et al. The role of cerebrospinal fluid 14-3-3 and other proteins in the diagnosis of sporadic Creutzfeldt-Jakob disease in the UK: a 10-year review. *J Neurol Neurosurg Psychiatry* 2010; **81:** 1243–48.

Neuro-oncology: continuing multidisciplinary progress

Progress has been slow in improving survival in patients with glioblastoma, the most fatal and frequent malignant brain tumour. However, since a phase 3 clinical trial[1] reported that use of temozolomide with and after radiotherapy was superior to radiotherapy alone, hopes have been raised for continued improvement, and as such, substantial steps were taken in 2010.

Standard care for patients with glioblastoma is temozolomide-based radiochemotherapy;[1] however, median overall survival is still about 15 months. Many new agents have been tested alone or as add-ons to the temozolomide regimen for improving outcome. One striking example is cilengitide, a novel integrin inhibitor, for which phase 1 and 2 studies of its use as a single agent in recurrent glioblastoma had shown good safety profiles and promising antitumour activity. Consequently, cilengitide was added to temozolomide with radiotherapy in a phase 1 and 2a study that showed that the combination was well tolerated, with median progression-free survival (PFS) and overall survival of 8 months and 16·1 months, respectively.[2] These survival benefits were increased in patients who had tumours in which the O6-methylguanine-DNA methyltransferase (*MGMT*) promoter was methylated. Cilengitide is now being studied in a randomised phase 3 trial (the CENTRIC study) as first-line chemoradiotherapy for patients with methylated *MGMT* promoters. Examples of the use of targeted therapies are the randomised phase 3 trials testing bevacizumab, a humanised monoclonal antibody against vascular endothelial growth factor (VEGF), in patients with newly-diagnosed glioblastoma, undertaken by the Radiation Therapy

Oncology Group (RTOG 0825 [NCT00884741]) and Roche (AVAglio [NCT00943826]), both of which are currently recruiting participants. These trials are based on the excellent overall response rate and PFS at 6 months (PFS-6) reported in the BRAIN study of bevacizumab for the treatment of patients with recurrent glioblastoma (long-term survival data were updated in 2010).[3]

Although the temozolomide regimen has antitumour activity, high-grade gliomas recur within a year, and treatment options are then limited. Temozolomide is a DNA alkylating agent that induces cytotoxic *O6*-methylguanine lesions in the DNA of tumour cells, which are effectively repaired by MGMT; in this way, the tumour cells eventually remove this cytotoxic DNA damage, leading to resistance to temozolomide. When repairing *O6*-methylguanine lesions, MGMT covalently accepts the methyl adduct to its active cysteine residue in a stoichiometric manner, thereby losing its enzymatic activity (that is the reason why MGMT is called a suicide enzyme); this process leads to a stage in which an increased dose of temozolomide might deplete MGMT activity and overcome temozolomide resistance. A phase 2 trial (the RESCUE study)[4] of continuous dose-dense temozolomide in patients with recurrent glioblastoma previously treated with a standard temozolomide regimen showed that continuous dose-dense temozolomide was well tolerated and resulted in a PFS-6 of 23·9%. Patients who had early recurrent glioblastoma during temozolomide cycles, and those who relapsed after completing adjuvant temozolomide, had higher PFS-6s of 27·3% and 35·7%, respectively, than did those who recurred on temozolomide for more than six adjuvant cycles, who had a PFS-6 of only 7·4%. These findings suggest that previous heavy exposure to temozolomide might hamper the efficacy of this strategy. Interestingly, PFS-6s were similar regardless of the methylation status of the *MGMT* promoter in these patients, perhaps suggesting that this regimen depletes MGMT. Whether continuous temozolomide is better than other dose-dense temozolomide regimens, such as the 7 days on and 7 days off (7/7) or the 21 of 28 days (21/28) regimens, needs to be determined. The DIRECTOR trial (NCT00941460) comparing efficacy between the 7/7 and the 21/28 regimens after failure of temozolomide in patients with recurrent tumours and the RTOG 0525 trial (NCT00304031), which is testing superiority of the standard 5/28 versus the 21/28 regimen in patients who were treated with concurrent temozolomide and radiotherapy, are ongoing and will be reported soon.

Accurate determination of the efficacy of new therapies needs well designed, widely accepted criteria for assessing tumour response and progression. The Macdonald criteria, using two-dimensional tumour measurements of the contrast-enhancing component of tumours, have been the gold standard.[5] However, there is increasing evidence that these criteria might be insufficient for assessing outcomes after radiochemotherapy (because of "pseudoprogression"), or after antiangiogenic therapy (because of "pseudoresponse"), and in patients with tumours that do not have a contrast-enhancing component. Therefore, the international Response Assessment in Neuro-Oncology (RANO) working group has been developing updated criteria to be used in clinical trials.[6] These criteria include definitions and guidance for the treatment of patients with measurable and non-measurable disease and those with multiple lesions, and strict rules for determining first progression and eligibility for enrolment in clinical trials; they also provide a more precise definition of treatment response, which incorporates MRI, non-enhancing disease, and clinical factors. The criteria will evolve to include diagnostic and neurocognitive measurements.

The Cancer Genome Atlas (TCGA) Research Network is generating a comprehensive catalogue of genomic abnormalities in glioblastoma.[7] In 2010, gene-expression profiling of 200 glioblastoma samples and two healthy brain samples identified four molecular subtypes: classic, proneural, neural, and mesenchymal, with differing genetic lesions and clinical behaviour.[8] Epigenetic analysis of methylation alterations in 272 glioblastomas identified a distinct molecular subgroup with hypermethylation at a large subset of genetic loci, thus named glioma-CpG island methylator phenotype (G-CIMP).[9] This feature, perhaps combined with other molecular characteristics, might prove to have diagnostic and prognostic value in future studies.

Patients with primary CNS lymphoma (PCNSL), a rare malignant brain tumour affecting elderly people, have poor survival, even after high-dose methotrexate (HD-MTX) followed by whole-brain radiotherapy (WBRT). Although this regimen may extend survival from 12–18 months to 30–60 months, it is associated with intolerable long-term neurotoxic effects. A

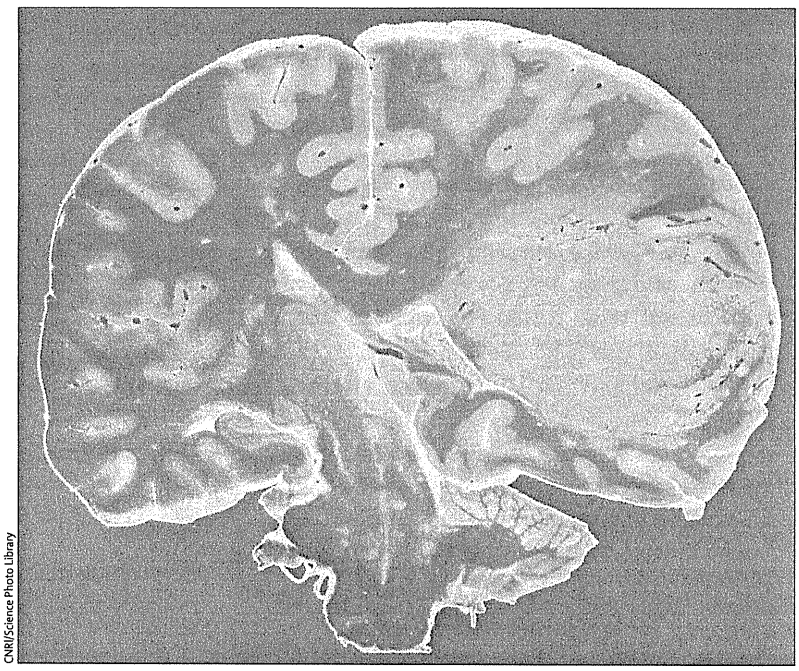

CNRI/Science Photo Library

randomised phase 3 clinical trial in 551 patients with PCNSL investigated the omission of WBRT from the first-line HD-MTX-based chemotherapy.[10] Although PFS was longer in patients treated with WBRT (but not statistically significant), median overall survival was similar in both treatment groups, with a lower incidence of treatment-related neurotoxic effects in complete responders when WBRT was omitted or delayed. These findings suggest that the gain of PFS by radiotherapy needs to be balanced against potential delayed cognitive dysfunction.

Neuro-oncology has become a prime example of a multidisciplinary field, which includes novel techniques in surgery, radiotherapy, targeted chemotherapies, drug delivery, and molecular genetics for a concerted onslaught on these devastating diseases. Achievements in bringing these new approaches into clinical trials over the past few years, especially in 2010, have shown acceleration towards truly personalised medicine that would previously not have been possible. Many of these trials are accruing patients now and will soon report their findings. We can look forward to these findings with great anticipation and the widely held conviction that these diseases can be beaten.

Motoo Nagane
Department of Neurosurgery, Kyorin University Faculty of Medicine, Mitaka, Tokyo 181-8611, Japan
nagane-nsu@umin.ac.jp

I declare that I have no conflicts of interest. I thank Prof Webster K Cavenee (Ludwig Institute for Cancer Research, San Diego, CA, USA) for critical reading of the commentary.

1 Stupp R, Mason WP, van den Bent MJ, et al, for the European Organisation for Research and Treatment of Cancer Brain Tumor and Radiotherapy Groups, and the National Cancer Institute of Canada Clinical Trials Group. Radiotherapy plus concomitant and adjuvant temozolomide for glioblastoma. *N Engl J Med* 2005; **352:** 987–96.
2 Stupp R, Hegi ME, Neyns B, et al. Phase I/IIa study of cilengitide and temozolomide with concomitant radiotherapy followed by cilengitide and temozolomide maintenance therapy in patients with newly diagnosed glioblastoma. *J Clin Oncol* 2010; **28:** 2712–18.
3 Friedman HS, Prados MD, Wen PY, et al. Bevacizumab alone and in combination with irinotecan in recurrent glioblastoma. *J Clin Oncol* 2009; **27:** 4733–40.
4 Perry JR, Bélanger K, Mason WP, et al. Phase II trial of continuous dose-intense temozolomide in recurrent malignant glioma: RESCUE study. *J Clin Oncol* 2010; **28:** 2051–57.
5 Macdonald DR, Cascino TL, Schold SC Jr, Cairncross JG. Response criteria for phase II studies of supratentorial malignant glioma. *J Clin Oncol* 1990; **8:** 1277–80.
6 Wen PY, Macdonald DR, Reardon DA, et al. Updated response assessment criteria for high-grade gliomas: response assessment in neuro-oncology working group. *J Clin Oncol* 2010; **28:** 1963–72.
7 Cancer Genome Atlas Research Network. Comprehensive genomic characterization defines human glioblastoma genes and core pathways. *Nature* 2008; **455:** 1061–68.
8 Verhaak RG, Hoadley KA, Purdom E, et al, for the Cancer Genome Atlas Research Network. Integrated genomic analysis identifies clinically relevant subtypes of glioblastoma characterized by abnormalities in PDGFRA, IDH1, EGFR, and NF1. *Cancer Cell* 2010; **17:** 98–110.
9 Noushmehr H, Weisenberger DJ, Diefes K, et al, for the Cancer Genome Atlas Research Network. Identification of a CpG island methylator phenotype that defines a distinct subgroup of glioma. *Cancer Cell* 2010; **17:** 510–22.
10 Thiel E, Korfel A, Martus P, et al. High-dose methotrexate with or without whole brain radiotherapy for primary CNS lymphoma (G-PCNSL-SG-1): a phase 3, randomised, non-inferiority trial. *Lancet Oncol* 2010; **11:** 1036–47.

1．高齢者初発膠芽腫に対する放射線化学療法の治療成績と因子解析

Combined radiochemotherapy for elderly patients with newly-diagnosed glioblastoma.
—Treatment outcome and analysis of prognostic factors—

永根　基雄　　小林　啓一　　林　　基高　　清水　早紀　　塩川　芳昭

[Purpose] To evaluate the efficacy of radiotherapy (RT) and adjuvant chemotherapy either consisting of ACNU-based regimen or temozolomide (TMZ) for elderly patients with newly diagnosed glioblastoma (GBM) since 2000.
[Patients and Methods] Thirty-two patients aged 65 years or older were treated with postoperative radiochemotherapy using either ACNU-based regimens or TMZ for newly diagnosed GBM. Median age at primary diagnosis was 73 years; 15 patients were male, 17 were female; median Karnofsky Performance Status (KPS) was 70 %. RT was applied with a median dose of 60 Gy. Four patients received ACNU monotherapy, 7 patients were treated with combined ACNU plus VP16, 13 with TMZ, and 8 patients underwent RT alone. Fourteen cases were treated by 2005, while 18 were treated after 2006. Overall survival (OS) and progression-free survival (PFS) were analyzed using a logrank test.
[Results] Median OS was 11.4 months (95% confidence interval [CI], 1.4～18.6) in all patients; median PFS (mPFS) was 4.1 months (95% CI, 3.2～4.9). Pretreatment KPS (≧ 70%, p=0.011), age (cutoff at 70 years) x treatment era (before 2005 vs. after 2006)(p=0.04), and TMZ/RT vs. RT alone (p=0.05) were significantly correlated with OS. MGMT status was also significantly associated with survival (p=0.05) among patients treated with chemotherapy, while it did not reach the significant level when all patients including those treated with RT alone were included (p=0.14). OS was not significantly different between patients treated with ACNU-based regimens and TMZ (p=0.93). In patients older than 70 years for whom ACNU was barely applied, TMZ was the favorable treatment over RT alone (p=0.06). At multivariate analysis, KPS (≧ 70%) and extent of resection (gross-total removal) were better independent prognostic factors for OS. No prognostic factors were significantly related to PFS, although there was a trend toward better survival by TMZ, followed by ACNU-based regimens over RT alone (p=0.09).
[Conclusions] Pretreatment PS, gross total removal, and MGMT status at chemotherapy were the significant prognostic factors for elderly patients with GBM. For those older than 70 years, the addition of TMZ to RT may improve survival.

杏林大学医学部　脳神経外科

Further prospective study is needed to evaluate the definite impact of TMZ and optimal RT dose in this cohort of patients.

はじめに

神経膠腫は原発性悪性脳腫瘍の代表疾患であるが，最も悪性度が高い膠芽腫（glioblastoma, GBM; WHO grade IV）は依然予後が極めて不良な難治性腫瘍である．現在の標準治療は安全な範囲での最大限の切除の後に放射線照射と化学療法を併用する集学的治療であり，初発膠芽腫に対しては，2005 年の European Organisation for Research and Treatment of Cancer（EORTC）と National Cancer Institute of Canada（NCIC）による多施設共同第 III 相臨床試験でテモゾロミド（temozolomide, TMZ）が有意に生存期間の延長に寄与することが示されて以降[1]，TMZ 併用放射線治療（RT）＋併用

Table 1 Patient Characteristics

Characteristic	Patients with GBM (Age ≥ 65) (N = 32) No.	%
Sex		
Male	15	46.9
Female	17	53.1
Age, years		
Mean	72.8	
Range	65-86	
Karnofsky Performance Scale		
Median	70	
Range	20-100	
Localization		
Frontal only	9	28.1
Other	23	71.9
Extent of resection		
GTR (100%)	13	40.6
PR	16	50.0
Biopsy	3	9.4
Chemotherapy (1st line)		
ACNU	4	12.5
ACNU+VP16	7	21.9
TMZ	13	40.6
MGMT gene promoter status		
Methylated	12	37.5
Unmethylated	12	37.5
Treatment era		
2000-2005	14	43.8
2006-2009	18	56.3

Abbreviations: GBM, glioblastoma; MGMT, O^6-methylguanine-DNA methyltransferase

後 TMZ 単独維持療法と考えられている．しかし，その試験での対象年齢は 70 歳以下であり，また一般に高齢者は化学療法への耐用性が低いことから，本疾患の高齢者に対する標準治療は十分に確立しているとは言えないのが現状である．

我々の施設では，本邦で TMZ が保険認可される以前には，70 歳以下の初発膠芽腫に対して ACNU 基盤の化学療法を施行してきたが，TMZ 認可後は TMZ の毒性が軽微なことから，70 歳以上の高齢者にも TMZ 療法を施行している．

今回，65 歳以上の初発膠芽腫症例に対し，ACNU 基盤治療時代と TMZ 認可後の初発膠芽腫に対する初期治療法による治療成績について因子解析を主に検討した．

1. 対象・方法

対象は，2000 年 4 月 ~2009 年 11 月までに杏林大学医学部附属病院にて術後初期治療が施行された 65 歳以上の初発膠芽腫 32 症例である．また，同期間中に治療された全膠芽腫 76 例とも比較検討した．

術後に全例放射線照射を 60Gy（2Gy/fr × 30）施行した．高齢者における radiation-induced delayed neurotoxicity を軽減する目的に，2009 年初頭からは，75 歳以上の症例には hypofractionation の照射法として 40Gy/15fr に変更した．化学療法に使用された治療レジメンは，① ACNU 単独療法（JCOG 0305 臨床試験の A 群を含む）が 4 例，② ACNU+VP16 併用療法が 7 例，③ TMZ 療法が

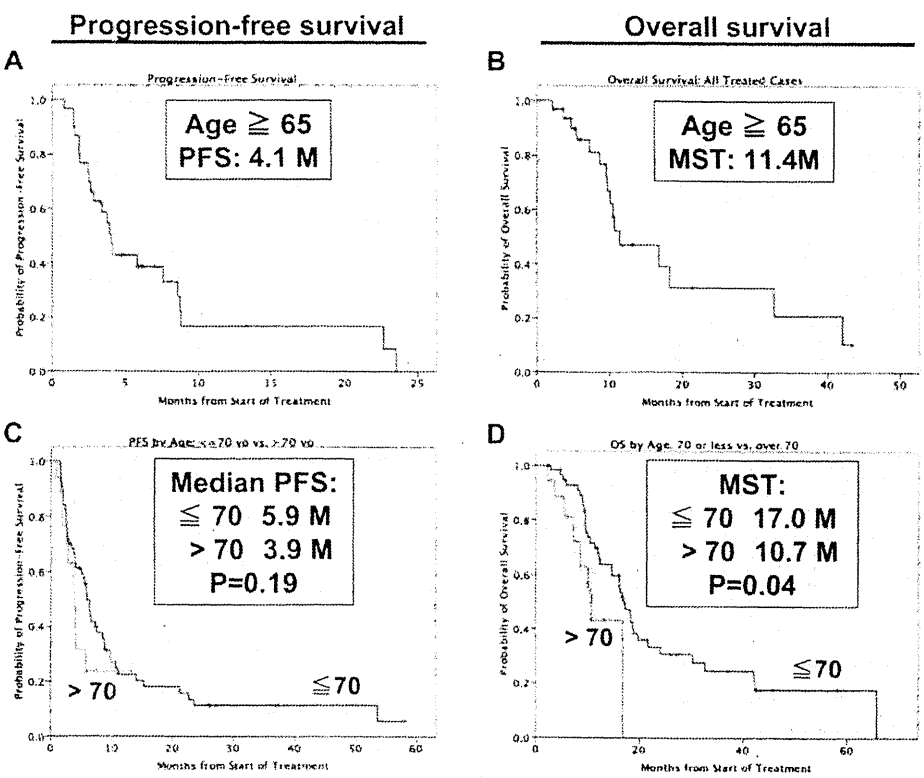

Fig. 1　Kaplan-Meier estimates of (A) progression-free survival (PFS) or (B) overall survival (OS) for all patients aged 65 years old or older, and (C) PFS or (D) OS according to age younger than 70 years or older.

13例，④化学療法なし（放射線治療単独）が8例であった．

解析項目は，全生存期間（overall survival, OS），無増悪生存期間（progression-free survival, PFS）をKaplan-Meier法にて解析し，有意差の有無をLogrank検定で行った．また，単変量解析にて有望な因子については，多変量解析（Cox proportional hazards）を加えて解析した．

2. 結　果

対象症例の背景因子：

症例全体で，性別は男性15例，女性17例，年齢は平均72.8歳（65~86歳），Karnofsky Performance Scale（KPS）は中間値70であった．手術での腫瘍摘出率は，全摘出（gross-total removal, GTR）（100%Gd造影部の摘出）が13例（40.6%），部分摘出（partial removal, PR）が16例

Table 2 Variables related to PFS and OS in patients with glioblastoma aged 65 or more: Univariate analysis

		PFS (months)			OS (months)		
Variable	n (event)	Median	95% CI	p*	Median	95% CI	p*
		4.1	3.2-4.9		11.4	4.1-18.6	
Age (y)							
≦70	14 (8)	7.6	0.0-15.8	0.57	18.2	0.0-37.2	0.13
>70	18 (8)	3.9	3.4-4.4		10.7	7.9-13.5	
Gender							
Male	15 (8)	3.8	2.5-5.0	0.77	10.7	9.4-12.0	0.94
Female	17 (8)	4.1	0.0-8.7		16.8	3.4-30.1	
Karnofsky Performance Scale							
≥70	16 (7)	4.1	0.9-7.3	0.127	18.2	0.0-42.4	0.011
<70	15 (9)	3.8	1.9-5.6		8.7	4.2-13.1	
Localization							
Frontal	9 (2)	7.6	2.5-12.7	0.53	16.8	8.7-24.8	0.23
Others	23 (14)	3.4	1.9-4.9		10.5	9.2-11.8	
Treatment era							
2000-2005	14 (9)	4.1	1.1-7.0	0.48	9.7	8.2-11.2	0.14
2006-2009	18 (7)	3.8	2.2-5.3		16.8	8.6-24.9	
Chemotherapy regimen							
ACNU-based	11 (8)	3.4	0.0-12.1	0.09	11.4	0.3-22.5	0.16
TMZ	13 (5)	7.6	1.0-14.2		16.8	7.0-26.6	
None (RT)	8 (3)	2.5	0.1-5.0		5.5	2.8-8.2	
Extent of resection							
GTR	13 (4)	4.1	0.0-8.6	0.65	42.1	-	0.07
Others	19 (12)	3.4	1.5-5.3		10.1	9.0-11.1	
MGMT status							
Methylated	12 (5)	7.6	0.0-24.3	0.13	32.6	0.3-64.9	0.04
Unmethylated	12 (8)	4.1	2.3-6.0		10.5	9.3-11.7	

Abbreviations: PFS, progression-free survival; MST, median survival time; GTR, gross total removal; TMZ, temozolomide; MGMT, *O*^{6}-methylguanine-DNA methyltransferase.
*Indicates log-rank.

(50.0%)，生検（biopsy）が3例（9.4%）であった（Table 1）．

生存率解析：

対象の32例のうち，PFSの解析が可能であった30例の中間PFS（mPFS）は4.1ヶ月（95%信頼期間 confidence interval, CI: 3.2~4.9）で，同期間中の全年齢膠芽腫74例での5.8ヶ月（95% CI: 3.9~7.7）に比べ短い傾向がみられた．全32例での中間OS（median survival time, MST）は11.4ヶ月（95% CI: 4.1~18.6）で，同期間中の76例での16.7ヶ月（95% CI: 14.2~19.2）より同様に短い傾向であった（Fig. 1）．この期間中全症例で，70歳以下（58例）と71歳以上（18例）の2群で比較すると，mPFSは5.9ヶ月 vs. 3.9ヶ月（p=0.187），MSTは17.0ヶ月 vs. 10.7ヶ月（p=0.044）とOSで有意に年少群での延長が認められた．

予後因子の単変量解析：

65歳以上の32症例を対象に，各予後関連臨床因子とO^6-methylguanine-DNA methyltransferase（MGMT）statusについて単変量解析を行った（Table 2）．PFSでは，化学療法の種類（ACNU基盤，TMZ，RT単独）でのTMZ群（p=0.09），MGMTがメチル化プロモーター群で延長する傾向（p=0.13）が認められた．OSでは，KPS（70以上），MGMT（メチル化＋）で有意な生存期間の延長がみられ（各p=0.011, 0.04），摘出率（GTR）も強い関連が認められた（p=0.07）（Fig. 2）．また，年齢（70歳以下），治療時期（2006年以降），化学療法種類でも延長する傾向が認められた（各p= 0.12, 0.14, 0.16）．

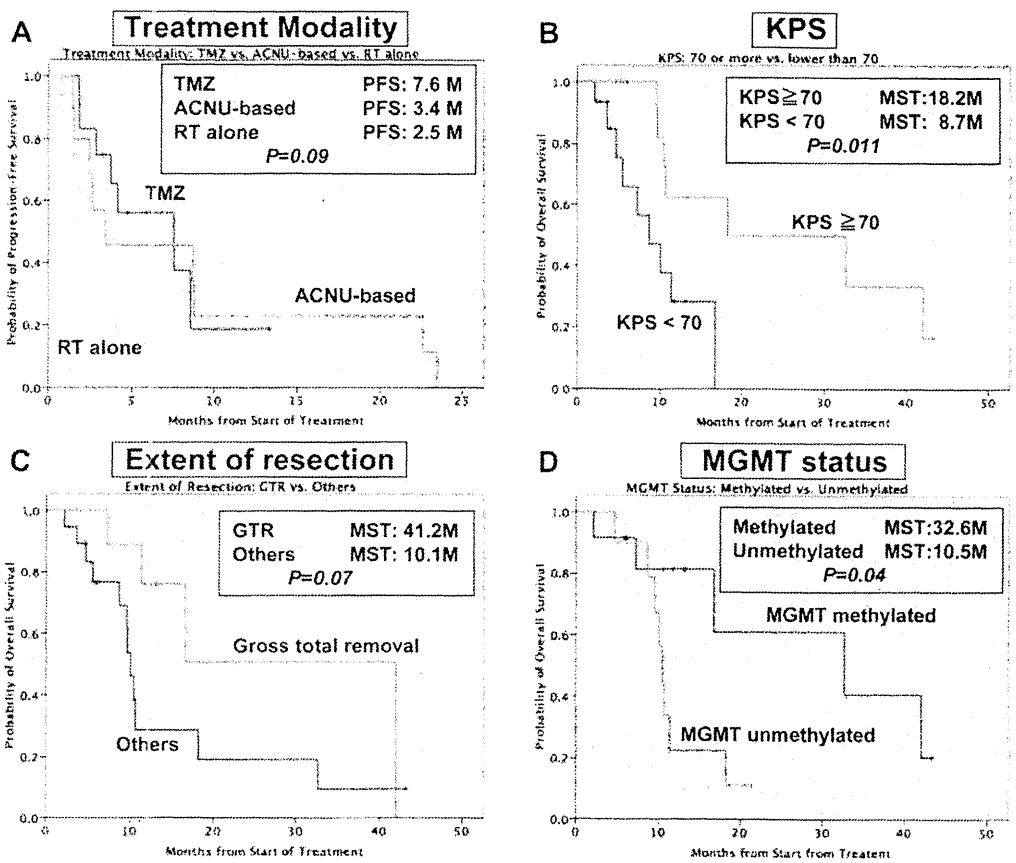

Fig. 2 Kaplan-Meier estimates of (A) progression-free survival according to the treatment modality, and overall survival according to KPS (B), extent of resection (C), or MGMT status (D).

更に，年齢 70 歳を境界として，2005 年まで（前期）と 2006 年以降（後期）の年代別での OS を比較すると，70 歳以下でも前期 11.4 ヶ月，後期 18.2 ヶ月と後期の方が良好であったが，71 歳以上では，前期 5.5 ヶ月，後期 16.8 ヶ月と大きく改善があり，全体で有意な差が示された（p=0.04）(Fig. 3A, B)．また，化学療法の種類間での比較では，TMZ 群と RT 単独群で MST 16.8 ヶ月 vs. 5.5 ヶ月と，TMZ 群が有意に延長した（p=0.050）．これを 71 歳以上の群に限定すると，TMZ 群は MST 16.8 ヶ月，RT 単独群は 5.5 ヶ月，p=0.06 とほぼ同様の結果であった（Fig. 3C, D）．一方，65 歳以上での ACNU 基盤治療群と TMZ 群では，MST が各 11.4 ヶ月 vs. 16.8 ヶ月と TMZ の方が良好であるが，p=0.93 であり有意差は認められていない．71 歳以上の高度高齢者では，TMZ 期以前は RT 単独療法がほとんどであり，ACNU 基盤療法施行例は僅少であったことを考慮すると，この結果から，TMZ 導入後は TMZ を RT と併用することで，特に 71 歳以上の高度高齢者における OS の改善に寄与していることが示唆される．

予後因子の多変量解析：

対象 32 症例で単変量解析にて，p<0.1 を示した因子について Cox proportion hazards 法による多変量解析を行った．PFS については化学療法の種類しか該当しなかったため，OS での KPS（70 以上），摘出率（GTR），MGMT（メチル化あり）の 3 項目について解析した．その結果 KPS70 以上（p=0.001, HR 13.9）と GTR（p=0.019, HR 6.5）が独立した有意な予後因子として抽出された．こ

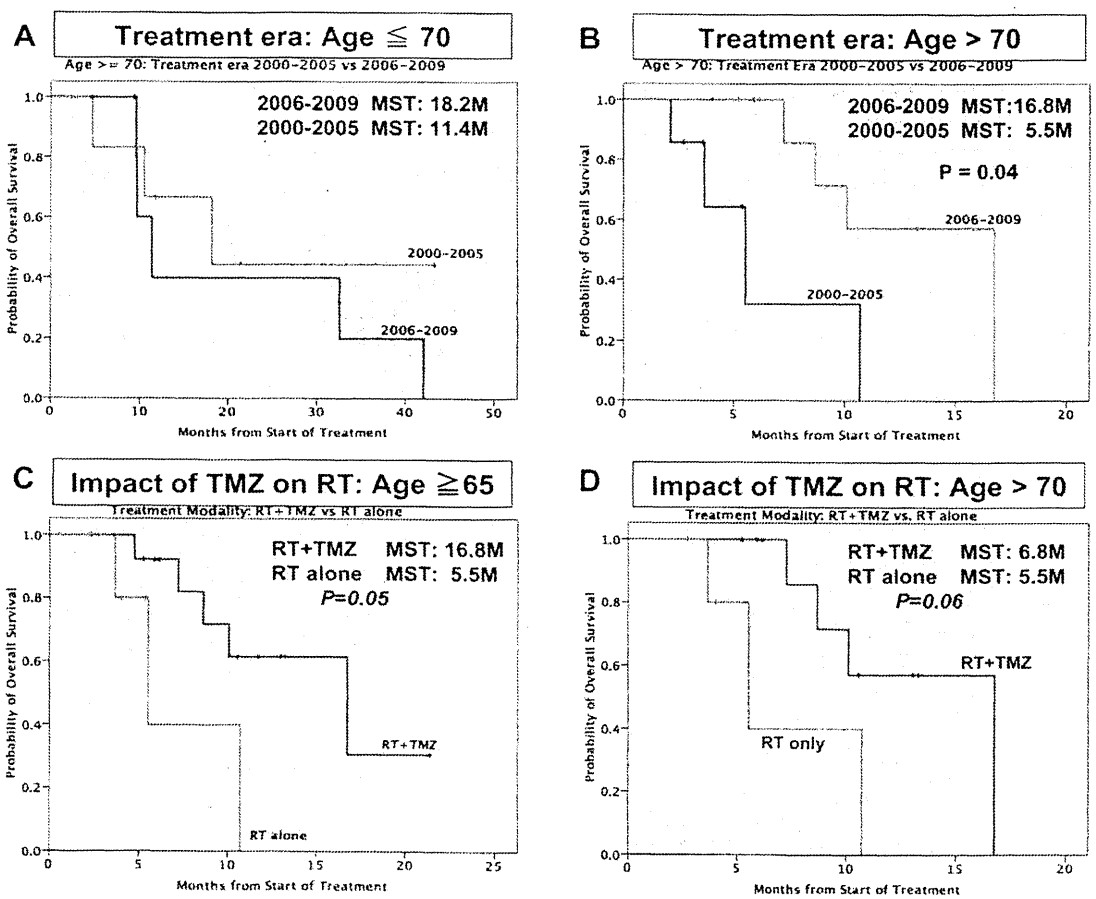

Fig. 3 Kaplan-Meier estimates of overall survival (OS) according to treatment era in patients aged 70 years or younger (A) or higher (B), and OS according to temozolomide treatment in patients aged 65–70 years (C), or older than 70 years (D).

の結果は，解析対象因子の有意水準を $p<0.2$ 以下としても同様であった．

3. 考　察

初発膠芽腫に対する標準治療は，2005 年以降従来の術後放射線照射 60Gy/30fr から，放射線治療に加えて TMZ を併用及び照射後単独維持療法を行う治療法へ世界的に変遷し，70 歳以下の症例では MST 14.7 ヶ月との結果が報告されている[1]．しかしこの試験も含め，一般に高齢者は身体条件が若年層症例に比べ劣り，特に全身への負担の多い化学療法の施行にはリスクが高まると考えられ，高齢者症例への化学療法の寄与度は低く，照射以外の有効な治療法がないため予後も更に不良と考えられている．

これまで施行されてきた臨床試験においても，年齢は 60 歳から 70 歳以上との設定で，MST は 5 ヶ月から 15 ヶ月と相対的に不良な結果が示されている[2-6]．特に TMZ の登場以前の放射線治療単独療法による治療では，MST は 5.1 ~ 7.3 ヶ月に留まっており，明らかに治療効果として十分ではない[2,6]．今回の検討でも，放射線治療単独での治療症例（計 8 例）の MST は 5.5 ヶ月であり，これまでの報告を裏付ける結果であった．このような状況下では，高齢者でより問題となり易い，放射線治療に伴う遅発性神経障害とそれに伴う ADL 低下を考慮した，低放射線線量との比較がランダム化試験で検討された．Roa らは 60 歳

Table 3　Variables related to OS in patients with glioblastoma aged 65 or more: Univariate analysis

Variable		n (event)	OS (months) Median	95% CI	p*
Age (y)					**0.04**
≦70					
	2000-2005	7 (5)	11.4	7.7-15.0	
	2006-2009	7 (3)	18.2	3.1-33.4	
＞70					
	2000-2005	7 (4)	5.5	2.7-8.4	
	2006-2009	11 (4)	16.8	-	
Chemotherapy					
ACNU-based		11 (8)	11.4	0.3-22.5	0.93
TMZ		13 (5)	16.8	7.0-26.6	
ACNU-based		11 (8)	11.4	0.3-22.5	0.15
None (RT)		8 (3)	5.5	2.8-8.2	
TMZ		**13 (5)**	**16.8**	**7.0-26.6**	**0.050**
None (RT)		**8 (3)**	**5.5**	**2.8-8.2**	
Age (y) ＞70					
TMZ		**10 (4)**	**16.8**	**-**	**0.06**
None (RT)		**7 (3)**	**5.5**	**2.8-8.2**	

*Indicates log-rank.

以上の膠芽腫症例で（65%で摘出術施行後），標準の60Gy/30frと低線量の40Gy/15frによる単独放射線治療では，MSTが前者で5.1ヶ月，後者で5.6ヶ月と有意差が認められないことを報告している[6]．我々の施設でも，高齢者膠芽腫症例に対する標準線量照射中からADLの著しい低下をきたした症例が続き，2009年以降は75歳以上では40Gy/15frの照射線量を採用している．

しかし，放射線治療単独療法での治療成績は明らかに不十分であり，化学療法併用の効果についても近年検討されてきている．Brandesらは65歳以上の膠芽腫症例（KPS ≧ 60，残存腫瘍≦ 2cm）に対し，摘出後60Gyの照射単独療法群と，照射後にPCV療法，あるいはTMZ療法を加えた治療群につき比較検討した．これら予後良好群症例ではTMZ治療群が最も良好な成績を示し，MST 14.9ヶ月，mPFS 10.7ヶ月であり，且つ高度血液毒性はPCV療法群より低頻度であった[7]．（放射線単独群では，各11.2ヶ月，5.3ヶ月，PCV療法群では，各12.7ヶ月，6.9ヶ月．）

EORTC/NCICの第III相試験においては，高齢になるほどTMZによる上乗せ効果が小さくなる傾向が示され，65歳以上（71歳まで）ではTMZ併用による生存率のhazard ratio（HR）は0.8に留まっている（全年齢では0.63）[5]．Combsらは65歳以上の初発膠芽腫（33%が生検術後）に対しTMZ併用照射を行い，MST 11.0ヶ月，mPFS 4ヶ月と報告している[3]．また，Minnitiらは，70歳以上のKPS 70以上の初発膠芽腫症例に対し60Gy照射＋TMZ及び6サイクルのTMZ維持療法を施行し，MST 10.6ヶ月，mPFS 7ヶ月であり，KPSが唯一の独立した予後因子であったと報告した[4]．更にBrandesらは65歳以上の予後良好群の症例（70歳以下が71%，KPS 80以上が92%，摘出以上が全例）に対する第II相試験で，TMZ併用放射線照射60Gyと維持TMZ療法（150mg/m2）を12サイクル施行し，MST 13.7ヶ月，mPFS 9.5ヶ月であった[2]．いずれも血液毒性は比較的軽度であり，PSが良好など予後良好な因子をもつ高齢者膠芽腫症例に対しては，従来の放射線治療単独よりTMZ併用療法の優位性が示唆された．今回の我々の症例では，術後TMZ併用放射線治療とその後のTMZ維持療法を施行した13例でのMSTは16.8ヶ月，mPFSは7.6ヶ月であり，これらの臨床試験の結果を支持する成績になっている．治療年代別での治療成績において，2005年までの症例と，TMZが認可された2006年以降の症例との比較では，特に70歳以上の高齢症例群で近年の方が生存予後良好であり（Table 3），これは2005年までは放射線治療単独が主であったのに対し，2006年以降はこの年代の症例に対してもTMZ併用療法を行うことが多くなったことと連関している可能性が考えられる．その意味で，TMZの登場は高齢者膠芽腫症例に対して治療上重要な貢献をしているとも考えられる．

TMZの治療効果を規定する因子としてMGMTが重要であり[8]，上記Brandesらの試験で高齢者膠芽腫の治療におけるMGMT statusの関与が検討された．全58例のうち，MGMT遺伝子プロモーター領域メチル化有り（methylated, M）が43%，メチル化なし（unmethylated, U）が57%であり，mPFSはM群で22.9ヶ月，U群で9.5ヶ月となり，M群で有意な延長が認められた（$p<0.005$），OSでは，M群は中間値に未達，U群では13.7ヶ月であり，同様にM群が有意に延長した（$p<0.01$））．多変量解析においてもMGMT statusは独立した有意な予後因子として抽出され，高齢者においても，MGMT statusがTMZ治療における重要な規定因子であることが検証された[2]．今回の解析では，OSにおける単変量解析にてMGMT statusは有意な因子となったが，多変量解析では独立した予後因子には残らず，KPSと摘出率のみが有意な因子であった．その理由としては今回の解析対象症例には放射線単独療法が施行された症例が含まれていることが挙げられ，またTMZ療法以外の化学療法も施行されており，特にMGMTと関連の薄いACNU以外の抗癌剤も併用されていたことなども影響しているものと考えられる．

高齢者に対する治療の影響として，Brandesらの試験では神経学的障害と認知障害が56%の症例で出現したが，放射線治療は標準量の60Gyが照射されていた[2]．神経毒性が出現するまでの中間期間は6ヶ月であり，同試験でのmPFSが9.5ヶ月であったことから，認められた神経症状の悪化

は腫瘍の増悪に由来するよりも，照射や化学療法などの治療が原因である可能性も否定はできない．先に述べた放射線照射線量の減量が，どの程度 TMZ 併用療法時に神経毒性の改善に寄与しえるか，まだ検証されていない．高齢者では特に神経機能障害が問題であり，高次脳機能検査や健康関連 QOL の調査を含めた検索が必要であり，今後はこれらのテストバッテリーを加えた各種治療方法による障害出現の評価を加えた prospective な試験を行うことが肝要である．

現在，高齢者初発膠芽腫に対して，短縮型放射線照射に TMZ 併用の有無による第 III 相試験が EORTC で施行中であり，その他 TMZ 単独療法の効果についても試験が行われている (ClinicalTrials.gov 参照)．今後，血管新生を標的とした bevacizumab などの分子標的治療薬が有害事象の観点からも検討される可能性もあり，予後が不良であるとされてきた高齢者膠芽腫に対する治療法がより改善されて行くことが期待される．

4. 結　語

2000 年以降に当院で経験した 65 歳以上の膠芽腫症例につき，その治療結果を報告した．高齢者膠芽腫の生命予後には，PS 及び MGMT status が有意な予後因子であり，高齢者に対しての TMZ 療法導入は，全体としての膠芽腫症例の生命予後改善に寄与する可能性があると考えられた．初期治療として ACNU 基盤治療法と TMZ 療法間には，現時点までは明らかな有意差が認められなかったが，前者は 70 歳以下でのみ施行されたのに対し，TMZ 療法は 70 歳以上でも施行されており，治療対象群の相違による可能性も考えられた．治療関連神経毒性の改善を目的とした放射線治療線量の適正化や，現在進行中の国際的臨床試験の結果，さらに分子標的治療薬など新規治療法の開発・導入により，高齢者膠芽腫治療にも新たな展開が生じる可能性が期待される．

文　献

1) Stupp R, Mason WP, van den Bent MJ, et al: Radiotherapy plus concomitant and adjuvant temozolomide for glioblastoma. N Engl J Med 352:987~96, 2005
2) Keime-Guibert F, Chinot O, Taillandier L, et al: Radiotherapy for glioblastoma in the elderly. N Engl J Med 356:1527~35, 2007
3) Combs SE, Wagner J, Bischof M, et al: Postoperative treatment of primary glioblastoma multiforme with radiation and concomitant temozolomide in elderly patients. Int J Radiat Oncol Biol Phys 70:987~92, 2008
4) Minniti G, De Sanctis V, Muni R, et al: Radiotherapy plus concomitant and adjuvant temozolomide for glioblastoma in elderly patients. J Neurooncol 88:97~103, 2008
5) Brandes AA, Franceschi E, Tosoni A, et al: Temozolomide concomitant and adjuvant to radiotherapy in elderly patients with glioblastoma: correlation with MGMT promoter methylation status. Cancer 115:3512~8, 2009
6) Roa W, Brasher PM, Bauman G, et al: Abbreviated course of radiation therapy in older patients with glioblastoma multiforme: a prospective randomized clinical trial. J Clin Oncol 22:1583~8, 2004
7) Brandes AA, Vastola F, Basso U, et al: A prospective study on glioblastoma in the elderly. Cancer 97:657~62, 2003
8) Hegi ME, Diserens AC, Gorlia T, et al: MGMT gene silencing and benefit from temozolomide in glioblastoma. N Engl J Med 352:997~1003, 2005

Neuro-Oncology Advance Access published February 11, 2010
Neuro-Oncology
doi:10.1093/neuonc/nop069

Predominant antitumor effects by fully human anti-TRAIL-receptor2 (DR5) monoclonal antibodies in human glioma cells in vitro and in vivo

Motoo Nagane, Saki Shimizu, Eiji Mori, Shiro Kataoka, and Yoshiaki Shiokawa

Department of Neurosurgery, Kyorin University Faculty of Medicine, Mitaka, Tokyo, Japan (M.N., S.S., Y.S.); Innovative Drug Research Laboratories, Research Division, Kyowa Hakko Kirin Co., Ltd, Takasaki, Gunma, Japan (E.M., S.K.)

Tumor necrosis factor–related apoptosis-inducing ligand (TRAIL/Apo2 L) preferentially induces apoptosis in human tumor cells through its cognate death receptors DR4 or DR5, thereby being investigated as a potential agent for cancer therapy. Here, we applied fully human anti-human TRAIL receptor monoclonal antibodies (mAbs) to specifically target one of death receptors for TRAIL in human glioma cells, which could also reduce potential TRAIL-induced toxicity in humans. Twelve human glioma cell lines treated with several fully human anti-human TRAIL receptor mAbs were sensitive to only anti-DR5 mAbs, whereas they were totally insensitive to anti-DR4 mAb. Treatment with anti-DR5 mAbs exerted rapid cytotoxicity and lead to apoptosis induction. The cellular sensitivity was closely associated with cell-surface expression of DR5. Expression of c-FLIP$_L$, Akt, and Cyclin D1 significantly correlated with sensitivity to anti-DR5 mAbs. Primary cultures of glioma cells were also relatively resistant to anti-DR5 mAbs, exhibiting both lower DR5 and higher c-FLIP$_L$ expression. Downregulation of c-FLIP$_L$ expression resulted in the sensitization of human glioma cells to anti-DR5 mAbs, whereas overexpression of c-FLIP$_L$ conferred resistance to anti-DR5 mAb. Treatment of tumor-burden nude mice with the direct agonist anti-DR5 mAb KMTR2 significantly suppressed growth of subcutaneous glioma xenografts leading to complete regression. Similarly, treatment of nude mice bearing intracerebral glioma xenografts with KMTR2 significantly elongated lifespan without tumor recurrence. These results suggest that DR5 is the predominant TRAIL receptor mediating apoptotic signals in human glioma cells, and sensitivity to anti-DR5 mAbs was determined at least in part by the expression level of c-FLIP$_L$ and Akt. Specific targeting of death receptor pathway through DR5 using fully human mAbs might provide a novel therapeutic strategy for intractable malignant gliomas.

Keywords: c-FLIP$_L$, glioblastoma, monoclonal antibody, TRAIL, TRAIL-R2/DR5

Malignant glioma, the most frequent primary intrinsic neoplasm arising in the central nervous system, remains incurable despite multimodal intensive treatments comprising maximum surgical resection, radiotherapy, and chemotherapy. Prognosis of patients with glioblastoma multiforme (GBM), the most malignant WHO grade IV glioma, has been dismal, with median survival time being only 12–15 months from initial diagnosis.[1] Chemotherapy only gives rise to a mild survival benefit using temozolomide given concomitantly with radiotherapy followed by adjuvant administration in patients with GBM;[2] thus novel therapeutic strategies which could exert robust tumoricidal activity have been required.

One such approach is to directly activate apoptosis pathways in tumor cells. Chemotherapy and ionizing irradiation trigger apoptosis by provoking the mitochondria-mediated "intrinsic" apoptosis pathway, which is regulated by the Bcl-2 family members and molecules involved in the downstream apoptosome.[3] Defects in the mitochondrial pathway may contribute to resistance to these conventional therapies. Activation of "death receptors" through oligomerization by their cognate trimeric ligands can also induce

Received June 5, 2009; accepted October 29, 2009.

Corresponding Author: Motoo Nagane, MD, PhD, Department of Neurosurgery, Kyorin University Faculty of Medicine, Mitaka, Tokyo 181-8611, Japan (nagane-nsu@umin.ac.jp).

tumor cell apoptosis through the "extrinsic" pathway.[4] Tumor necrosis factor (TNF)-related apoptosis-inducing ligand (TRAIL) (also called Apo2 L) is a member of the TNF superfamily which includes FasL (CD95 L) and TNF-α. TRAIL binds to its cognate death receptors, DR4 (TRAIL-R1)[5] and DR5 (Killer/TRAIL-R2/TRICK2)[6,7] containing a death domain (DD) in their cytoplasmic domain, and is capable of inducing rapid apoptosis through the activation of caspases, a family of cysteine proteases, in tumor cells of diverse origins, but not in most normal cells including astrocytes *in vitro*,[8–13] thereby being investigated as a potential agent for cancer therapy.[14]

Besides death-inducing TRAIL receptors DR4 and DR5, there are 3 other receptors, DcR1 (TRID/TRAIL-R3),[6,7] DcR2 (TRUNDD/TRAIL-R4),[15,16] and osteoprotegerin[17] acting as decoy receptors by competing with DR4 or DR5 for binding to TRAIL. DR4 and DR5 transcripts are expressed in some glioma cells, while at a low level in the brain.[5,7,11,18] Activation of DR4 and/or DR5 causes recruitment of adaptor molecules, preferentially fas-associated death domain protein (FADD), through their DD interaction, which in turn activates the initiator caspase-8 or -10 through their death effector domains (DEDs) (formation of death-inducing signaling complex; DISC).[19] This leads to direct activation of the effector caspase-3 or -7 and subsequent progression of irreversible cell death processes. TRAIL may also activate intrinsic mitochondrial apoptosis pathways to variable extents through caspase-8-mediated cleavage of cross-talk protein Bid, where cytochrome c release from mitochondria leads to the formation of the "apoptosome" with Apaf-1, dATP, and procaspase-9, resulting in the activation of an initiator caspase-9 and subsequent progression of the caspase cascade.[20,21] Molecules acting on these pathways may confer resistance to TRAIL-induced apoptosis when inadequately expressed. These include reduced expression of FADD, caspase-8, as well as increased expression of TRAIL decoy receptors and intrinsic apoptosis inhibitors, c-FLICE inhibitory protein (FLIP), XIAP, Bcl-2 family members, PEA-15, upregulated Akt and nuclear factor kappa B (NF-κB) signaling, and caspase mutations.[22–31]

In human glioma cells, a recombinant soluble form of TRAIL (sTRAIL) induces rapid and significant apoptosis, and its cytotoxic activity can be further enhanced by combination use of chemotherapeutic agent cisplatin or ionizing irradiation.[9,32] Importantly, systemic administration of human sTRAIL has shown a reasonably safety profile in mice or nonhuman primates,[8,33] and furthermore, treatment with the untagged, trimeric sTRAIL has shown no cytotoxicity on human hepatocytes or keratinocytes.[34,35] The potential clinical use of sTRAIL has been investigated in clinical trials (Phase II) (Genentech homepage).

Alternative approaches to activate the TRAIL pathway include the use of specific agonistic antibodies[36,37] that exploit the receptor discriminating specificity and prolonged bioavailability of IgG. Monoclonal antibodies (mAbs) are now widely applied clinically for cancer therapy; for instance, rituximab, an anti-CD20 mAb for CD20-positive non-Hodgkin B-cell lymphomas, trastuzumab, an anti-Her2/ErbB2 mAb for breast cancers, and bevacizumab, an anti-VEGF mAb for colorectal cancers. Among several types of recent therapeutic mAbs, fully human mAbs have a discrete advantage that they would evade the potential immunological response against the introduced antibody, compared with other mAbs carrying mouse sequences, which could be still immunogenic as fully mouse mAbs. We have generated fully human mAbs to DR4 or DR5 (IgG class), which are specifically bound to the ectodomain of the receptors,[38] thereby potently induced the death of cancer cells in vitro.[38] A direct agonist mAb to DR5, KMTR2, could suppress the growth of human colon cancer xenografts in vivo without antibody crosslinking,[39] independent of host effector function.

These observations prompted us to test whether a fully human anti-TRAIL receptor mAb could effectively induce glioma cell death. Here, we show that DR5 is the predominant TRAIL receptor, which is expressed at the cell surface and mediates apoptotic signals in human glioma cells. Sensitivity of human glioma cells to anti-DR5 mAbs might be determined at least in part by the expression level of c-FLIP$_L$ and Akt. Anti-DR5 mAbs exert antitumor effects both in vitro and in vivo. Our results suggest that specific targeting of the death receptor pathway through DR5 using a fully human mAbs might provide a novel therapeutic strategy for intractable malignant gliomas.

Materials and Methods

Reagents

Soluble human recombinant FLAG-TRAIL was prepared as previously described[9] and was stored at −80°C. Anti-FLAG monoclonal antibody (mAb) M2 was obtained from Sigma.

Monoclonal Antibodies

Fully human anti-human DR4 mAb, B12, and anti-DR5 mAb, E11, H48, and KMTR2, were described elsewhere.[38,39] These mAbs, except KMTR2, require crosslinking with anti-human IgG to be fully active apoptosis inducers. KMTR2 clusters DR5 on the cell surface, thereby inducing apoptosis with or without crosslinking.[39]

Cells

The human glioma cell lines used were described previously[32] and were cultured as described.[40] A tumorigenic subpopulation of the T98G cell line, designated T98SQ1, was generated by re-culturing in dish of a T98G xenograft that was established in a nude mouse. Normal human astrocytes (NHA) were purchased from Cambrex (Walkersville, MD), and cultivated in AGM medium per the manufacturer's recommendation. Primary cultures of glioma cells were established by

transferring tumor tissues in DMEM growth medium supplemented with 10% FBS immediately after resection, thereafter they were mechanically dispersed and plated into T75 flasks and incubated in DMEM supplemented with 10% FBS, 2 mM glutamine, 100 U/mL penicillin, and 100 μg/mL streptomycin in a humidified atmosphere of 5% CO2 at 37°C. The culture medium was changed every 3–4 days. When cells reached subconfluence, they were passaged using trypsin digestion. Malignant gliomas were surgically removed at Kyorin University Hospital. Patient material was obtained with informed consent and approval from the Institutional Ethics Committee.

Plasmids and Transfection

The plasmid encoding human c-FLIP$_L$ and c-FLIP$_S$, pCR3.V64-Met-Flag-FLIP$_L$ and pCR3.V62-Met-Flag-FLIP$_S$, respectively, were kind gifts from Dr. Jurg Tschopp (University of Lausanne). The empty vector pCR3.neo was generated by removing an *Eco*RI fragment from the pCR3.V62-Met-Flag-FLIP$_S$ plasmid. Cells were transfected with these plasmids using the calcium phosphate precipitation method and selected in the presence of G418 (Gibco/BRL) to establish G418-resistant subclones, including those expressing high levels of c-FLIP$_L$.

Western Blotting

Whole cell lysates were prepared in RIPA buffer and were subjected to Western blot analyses as previously described.[40] Proteins on the polyvinylidene difluoride (PVDF) membranes were probed with antibodies against DR5 (polyclonal, R&D Systems), DR4 (polyclonal, BD PharMingen), DcR1 (Imgenex), DcR2 (polyclonal, Imgenex), FADD (monoclonal, BD Transduction), c-FLIP (monoclonal, ALEXIS Biochemicals), caspase-8 (polyclonal, BD PharMingen), caspase-9 (monoclonal, Trevigen), caspase-3, cleaved caspase-3 (Cell Signaling Technology), XIAP (BD Transduction Laboratories), Apaf-1 (Transduction Laboratories), Akt (Cell Signaling), Survivin (Cell Signaling), Cyclin D1 (NeoMarkers), Bax (Ab-1, NeoMarkers), Bak (Ab-1, Oncogene), Bid (polyclonal, BD PharMingen), Bcl-2 (Ab-1, NeoMarkers), Bcl-X$_L$ (polyclonal, BD Transduction), poly(ADP-ribose) polymerase (PARP) (C2-10; Enzyme System Products), and detected by chemiluminescence and quantified (LAS 1000, Fuji). Loading of lysates on membranes was evaluated by β-actin blot.

Flow Cytometry

For the detection of cell surface TRAIL receptors, cells (~1 × 10^6 cells/sample) were washed with PBS containing 1% FBS and 0.05% NaN_3 and were stained with phycoerythrin (PE)-labeled mouse monoclonal anti-human DR4 or DR5 (eBioscience) on ice for 1 hour. After washing, cells were analyzed by on flow cytometry (FACScan, BD).[38] For apoptosis assays, cells were plated overnight and treated for 48 hours. Cells were then collected, fixed in 4% paraformaldehyde and permeabilized in 0.1% Triton-X in 0.1% sodium citrate solution, followed by incubation with terminal deoxynucleotidyl transferase-mediated nick end labeling (TUNEL) solution (Roche) at 37°C for 1 hour. TUNEL-positive cells stained with fluorescein were analyzed by flow cytometry using Cell Quest software.

Growth Inhibition Assays

Cytotoxicity was evaluated using the 3-(4,5-dimethylthiazol-2-yl)-2,5-diphenyl tetrazolium bromide (MTT) survival assays as described.[32] Briefly, cells were plated at 1 × 10^4 cells/well in 96-well microtiter plates overnight. Cells were then treated with 200 μL fresh medium containing drugs, cultured for 48 hours followed by an additional 4 hours with 250 μg/mL MTT, and analyzed using a microplate reader (Molecular Devices). The effects of treatment are expressed as percentage of growth inhibition using untreated cells as the uninhibited control.

TUNEL Assays

Apoptotic cell death was determined by TUNEL assays using In Situ Cell Death Detection Kits (Roche) as described.[40]

siRNA Treatment

A double-stranded siRNA oligonucleotide mixture against c-FLIP$_L$ was purchased from Dharmacon (siGENOME SMARTpool; Dharmacon RNA Technologies). siRNA for nonsilencing control (nontargeting siRNA) (siCtl) is an irrelevant siRNA with random nucleotides and no known specificity. c-FLIP$_L$-siRNA (0.1 μM) or nontargeting siRNA (0.1 μM) was transfected into glioma cells using DharmaFECT, and the cells were used for experiments 24–72 hours after transfection.

In Vivo Study

Human glioma cells (2 × 10^6 cells) were suspended in 0.1 mL PBS and injected subcutaneously into the right flank of 4- to 5-week-old female nude mice of BALB/CA background (Saitama Experimental Animals Supply, Co. Ltd.). For the treatment of the established xenografts, the tumors were permitted to establish and grow for 20 days (tumor volume ~120 mm^3). For intracerebral stereotactic inoculation, 5 × 10^5 glioma cells in 5 μL of PBS were inoculated into the right corpus striatum of the mouse brain as described.[40] Either anti-DR5 mAb (5 mg/kg) or control nonspecific human IgG (DNP) was administered i.p. daily for 3 consecutive days. The growth of tumors was measured as described.[41] Systemic toxicity of the treatments was assessed by change in body weight and by organ inspection at

autopsy. Mice were sacrificed by CO_2 inhalation when they became moribund. All animal procedures were approved by the Animal Care and Use Committee of the Kyorin University Faculty of Medicine.

Statistical Analysis

The data were analyzed for significance by Mann–Whitney's *U*-test or Student's *t*-test. Correlation was analyzed using Spearman's rank correlation test. Survival of mice bearing intracerebral xenografts was calculated according to the Kaplan–Meier method, and differences in survival were evaluated with the log-rank test. All statistical analyses were done using the statistical package SPSS 17.0J (SPSS, Inc.).

Results

Fully Human Anti-human DR5 mAbs Induce Apoptosis in Human Glioma Cells

We first sought to determine whether specific targeting of cell surface TRAIL receptors by anti-TRAIL receptor mAbs could induce cytotoxic effects in 12 human glioma cell lines. The anti-TRAIL receptor mAbs, B12 or E11, H48, and KMTR2, have been previously shown to bind specifically to their cognate receptor, either DR4 (B12) or DR5 (E11, H48, and KMTR2), respectively.[38,39] Soluble FLAG-tagged TRAIL (sTRAIL) with crosslinkers effectively killed the majority of human glioma cell lines with IC_{50} values lower than 0.1 μg/mL. Similarly, treatment with either anti-DR5 mAb E11 or H48 resulted in significant cytotoxicity in the presence of crosslinking anti-human IgG antibody in 8 of 12 glioma cell lines (Fig. 1). This was accompanied by changes in morphology typical of apoptotic cell death, which was confirmed by DNA fragmentation detected by TUNEL assays (Fig. 2). Furthermore, treatment with anti-DR5 mAbs lead to cleavage and activation of caspase-8, -9, and -3, as well as Bid, which results in the cleavage of PARP, an intrinsic substrate for executioner caspase-3 (data not shown). The cytotoxicity was abrogated in the presence of TRAIL-neutralizing DR5-Fc (data not shown), suggesting that the binding of antibody to DR5 is essential for the antibody-mediated effects.

The profiles of cell lines sensitive to anti-DR5 mAbs were identical to that to sTRAIL. IC_{50} values of sensitive cells, such as T98G, SF188, LNZ308, U87MG, and U251MG, were also lower than 0.1 μg/mL (Table 1). KMTR2 induced cell death effectively in T98G, SF188, and U87MG cells, even in the absence of crosslinkers. In contrast, glioma cells were totally insensitive to treatment with anti-DR4 mAb B12 (Fig. 1). These results suggest that TRAIL induces apoptosis predominantly through the DR5-mediated pathway but not DR4 in human glioma cells.

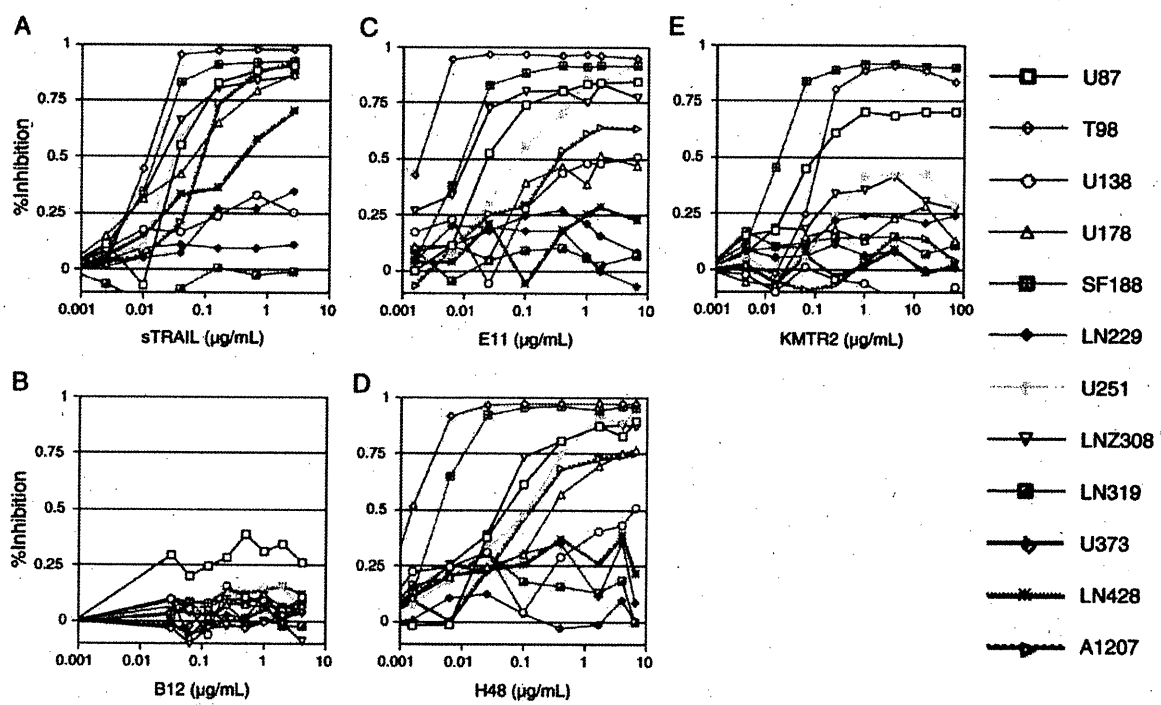

Fig. 1. Cytotoxic effects of soluble TRAIL (A) and fully human mAbs against DR4 (B12, B) and DR5 (E11, C; H48, D; KMTR2, E) in a panel of human glioma cell lines. Cells were treated for 48 hours with either sTRAIL, B12, E11, or H48 in the presence of antibodies for crosslinking, or KMTR2 in the absence of crosslinkers, at doses indicated at the bottom of each panel. Cytotoxicity was determined by MTT assays. Results were reproduced in 2 or more independent experiments; values are expressed as the mean of triplicate wells; bars, SD.

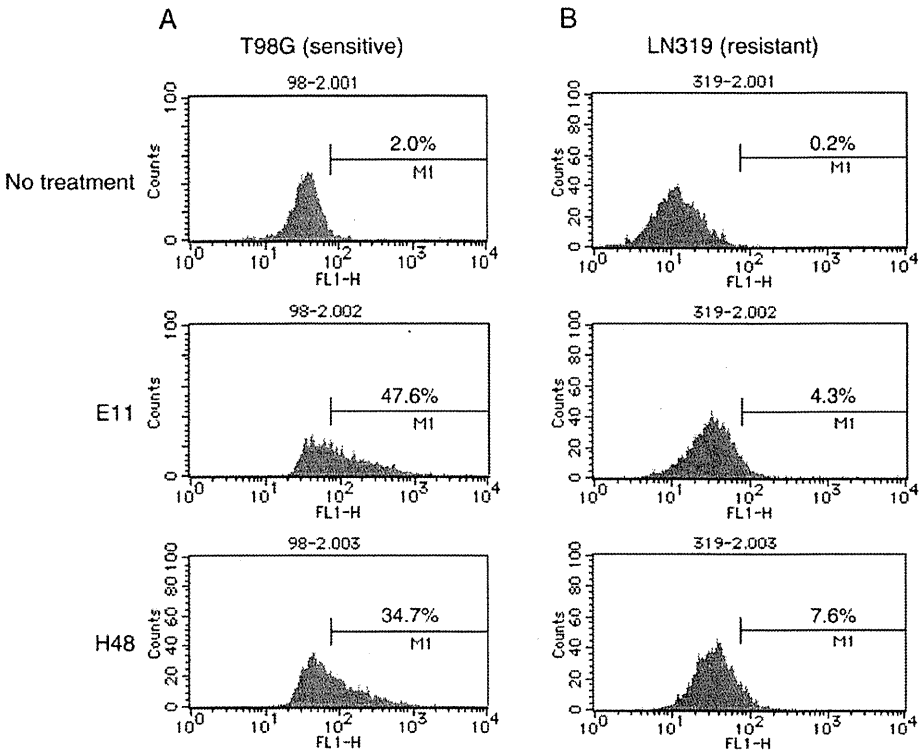

Fig. 2. Fully human anti-DR5 mAbs induced apoptosis in human glioma cells. TRAIL-sensitive T98G (A) and TRAIL-resistant LN319 (B) cells were treated with or without anti-DR5 mAbs E11 or H48 (0.1 μg/mL). After 48 hours treatment, cells were fixed, permeabilized, and stained for TUNEL, followed by flow cytometry analysis. The percentage of TUNEL-positive cells (fluorescein-positive) is indicated on each graph.

Table 1. IC_{50} values for TRAIL and anti-TRAIL receptor mAbs in human glioma cell lines

Cell line	sTRAIL	E11	H48	B12
U87	0.036	0.024	0.064	H
T98	0.013	0.002	0.001	H
U138	H	4	6	H
U178	0.079	1.519	0.319	H
SF188	0.019	0.011	0.005	H
LN229	H	H	H	H
U251	0.035	0.083	0.129	H
LNZ308	0.0252	0.014	0.049	H
LN319	H	H	H	H
U373	H	H	H	H
LN428	0.46	H	H	H
A1207	0.106	0.014	0.147	H
(μg/mL)	H: >2.56	H: >6.4	H: >6.4	H: >4.0

Anti-DR5 mAbs Did Not Affect the Viability of NHA

We next examined the effects of the treatments on NHA. Treatments with anti-DR5 mAbs, E11, H48, and KMTR2, and anti-DR4 mAb B12 did not cause cytotoxicity in these cells, even at a high concentration (10 μg/mL), whereas treatment of LNZ308 cells, a positive control of the treatment, did show the expected cytotoxicity (Fig. 3), indicating that NHA are insensitive to the mAb treatment.

Molecular Determinants of Sensitivity to Anti-DR5 mAbs

We next sought to determine which key molecules working in the apoptosis-inducing pathways are responsible for sensitivity to anti-DR5 mAb in human glioma cells. As we have demonstrated that the proapoptotic TRAIL-specific receptor DR5 was upregulated by both DNA damaging chemotherapeutic drugs and ionizing irradiation, thereby mediating enhancing TRAIL sensitivity in human glioma cells,[9,32] we examined the cell surface expression of DR5 by flow cytometry as well as its whole cellular expression by Western blot. The DR5 cell surface expression level, but not its whole cellular expression level, was weakly associated with the sensitivity of glioma cells to anti-DR5 mAbs (E11: $P = .145$, H48: $P = .118$, Spearman's rank correlation) (Fig. 4A and Table 1).

Among molecules downstream to DR5, the expression of an intrinsic apoptosis inhibitor c-$FLIP_L$ was almost undetectable in highly sensitive T98G and SF188 glioma cell lines, and its expression level significantly correlated with sensitivity to anti-DR5 mAbs (E11: $P = .003$, H48: $P = .006$, sTRAIL: $P = .008$ Spearman's rank correlation) (Fig. 4B). In contrast, expression of the alternative spliced form c-$FLIP_S$ was undetectable in all 12 human glioma cell lines tested (positive control of the Western blot was T98G.FLIPs cells). FADD, another key molecule in DISC, and Bcl-2